

Morphological and climate balance: Proposal for a method to analyze neighborhood urban forms by way of densification



Martina Pacifici^{a,*}, Karin Regina de Castro Marins^a, Vinicius de Mello Catto^a, Fabrizio Rama^b, Quentin Lamour^a

^a School of Engineering of the University of São Paulo, Department of Construction Engineering, Prof. Almeida Prado Avenue, Alley 02, No. 83, 05508070, São Paulo, SP, Brazil

^b School of Engineering of the Federal University of Santa Catarina, Department of Sanitary and Environmental Engineering, Campus Reitor João David Ferreira Lima, s/n, Trindade, 88040-900, Florianópolis, SC, Brazil

ARTICLE INFO

Keywords:

Urban morphology
Urban climate
Assessment method
Compact cities
Built and open spaces
Neighborhood scale

ABSTRACT

The major cities in the world have adopted certain strategies for people densification to optimize transport costs, to multiply exchanges of goods, to maximize social networking, as well as to promote economic growth. The implementation of such compact cities has profoundly affected the livability of public spaces and the comfort of pedestrians so far. In order to assess the environmental sustainability of this process, a method of analysis is proposed and applied at a local scale. Combining a morphological and climate site assessment, the method is addressed to urban areas affected by a process of built densification or relevant changes. A case study was performed in São Paulo, in an urban area of 100 ha. Inside this domain, different climatic and morphological environments were selected to perform a more detailed comparative analysis of the samples chosen. Climate variability was observed in various points of the domain, despite their very close distances. Three climate zones were identified and morphologically described. The results showed an effective correlation between the spatial arrangement of urban cross-sections and the related climate conditions at the neighborhood level; as a consequence, they could contribute to facing the issue of Compact City Design, improving its environmental performance.

1. Introduction

Cities are hybrid spaces, in which the natural environment blends with the built form produced by man. The complex interaction of these two components discerns an urban settlement from another, providing a new form of “anthropic diversity”. The way in which built spaces are organized and fit into the original geographical context is critical. According to Soleymanpour, Parsaee, and Banaei (2015), people’s comfort and satisfaction depend on the accommodation of built products within the local microclimate; a significant distance divides the modern and the traditional city; while the first one increasingly worsens the climate context, the second one was able to enrich it.

The industrial revolution is a significant step that universally brands the transition from small urban centers to great modern cities (Marx, 1967 *apud* Harvey, 2005). Since then, new patterns of urban growth have emerged; they diverge from the historical urban fabric and modify the spatial proportionality between built forms. Consequently, the ancient spatial arrangements, resilient and capable of favoring good

microclimate benefits, disappear from the modern fabric, replaced by a monotone design that disregards the original environmental context.

Along this process, the “dichotomy of human and natural systems” increases (Barau, Maconachie, Ludin, & Abdulhamid, 2014) and the urban development is transformed “in an accumulation of disconnected and fragmented regions” in which mega-objects remain “detached from any urban fluidity” (Suau, Bugarič, & Fikfak, 2015). According to Harvey (2005), capital accumulation permanently transforms the anthropic and natural environment, resulting in morphological changes, causing continuous expansion of the traditional historic centers and creating the emergence of “new spatial structures” (Harvey, 2005).

Examples of urban spatial structures, currently emerging in some cities throughout the world, have resulted from the implementation of Transit-Oriented Development (TOD) strategies, that intend to “reduce automobile use and promote the use of public transit and human-powered transportation modes through high density, mixed use, environmentally-friendly development within areas of walking distance from transit centers” (Sung & Oh, 2011). Many American and European

* Corresponding author.

E-mail addresses: martinapacifici@usp.br (M. Pacifici), karin.marins@poli.usp.br (K.R.d.C. Marins), vinicius.catto.96@gmail.com (V.d.M. Catto), fabriziorama@hotmail.com (F. Rama), quentin.lamour@usp.br (Q. Lamour).

<http://dx.doi.org/10.1016/j.scs.2017.07.023>

Received 22 August 2016; Received in revised form 26 June 2017; Accepted 30 July 2017

Available online 05 August 2017

2210-6707/ © 2017 Elsevier Ltd. All rights reserved.

cities have incorporated TOD concepts in their planning by inducing high-density development along the transportation lines (UN-Habitat Core Team, 2016). Besides the benefits described above, the strategy has controversial purposes; if on the one hand, TOD aims to content the human and urban form dispersion, on the other hand, it creates a permanent infrastructure which increases the exchange points at the service of a production system, thus supporting a geographical urban expansion. This type of urban planning induces a morphological fabric transformation around the new transport axes. The resulting spatial structure shares common features characterized by: (a) *People Densification*, (b) *Land Use Change*, (c) *Built Compactness*, (d) *Verticalization*, (e) *Closed Accessing*, (f) *Urban Form Homologation*.

The first feature, *People Densification*, consists in gathering people in order to prevent scattered urban settlements; the second, *Land Use Change*, allows constraining the constructed density around transit, by applying an appropriate policy (Suzuki, Cervero, & Iuchi, 2013); the third, *Built Compactness*, encourages the maximum exploitation of the land value; the fourth, *Verticalization*, favors a high-plot-ratio with low-site-coverage (Zhu, 2012); the fifth, *Closed Accessing*, prevents the lot access at the ground level, delegating their security to hired security force (Newman, 1996); the last one, *Urban Form Homologation*, encloses the high diversity of traditional urban forms into a low-diversity, simplified, and increasingly anthropogenic urban landscape (Salvati, Smiraglia, Bajocco, & Munafò, 2014).

The six phenomena described above, mixed among them, result in new dense spatial structures, besides built and unbuilt spaces proportions that produce various climate effects. First of all, the increase of physical obstructions restricts the longwave radiative heat loss and enhances the rise of anthropogenic processes. These facts favor the release of excess heat in the air; the urban temperature rises and becomes higher than the countryside surroundings, resulting in the Urban Heat Island Effect (Unger, 2004). Simultaneously, by increasing the plot ratio and the land coverage, the daylight availability on building facade and the openness of sky view at the ground level decrease (Cheng, Steemers, Montavon, & Compagnon, 2006). In addition, the increase of the built mass, carried by TOD, entails more materials to be used for coat facades, roofing, to equip transport corridors, and to supply them with urban furniture. For Erell, Pearlmutter, and Williamson (2011), the absorptivity and thermal admittance of these surface materials have a significant impact on the thermal and hydrological balance of a city. At the pedestrian scale, the materials switch radiant exchanges with people, affecting their thermal comfort.

Besides, urban built densification and air quality are closely related, as the dispersion of atmospheric pollutants is constrained by the built morphology. São Paulo, especially, falls into the ranking of the most polluted mega cities (WHO, 2016), in which the main sources of pollutant emissions are caused by motor vehicles (Jacobi & Macedo, 2000). High densities favor pollution concentration; consequently, “uniformity in building height, canyon width and canyon length should be avoided. Non-uniformly constructed roof height provides better ventilation” (Erell et al., 2011). According to Xie, Huang, Wang, and Xie (2005), variations in solar heating on the urban surfaces leads to a strong buoyancy force close to surfaces, largely influencing the air motion and the pollutant dispersion in the canyon.

At the pedestrian-level, as in Yuan and Ng (2012), “the urban ventilation performance mostly depends on the pedestrian-level building porosity”; porosity is obtained by decreasing the site coverage, increasing wind permeability in the podium layer, and opening air passages at the ground level and not along the tower height, planning building setback and separations between blocks.

Finally, in terms of daylighting, compact building structures could cause solar obstruction towards the low-rise fabrics. In this regard, Knowles and Berry (1980) were concerned with the Los Angeles new developments which, by introducing high-rise buildings, cast long shadows over the northern single family houses. According to the authors, these actions restrict the right to solar access, impacting the

neighborhood quality of life, as well as compromising their potential of energy conversion. Conversely, Emmanuel, Rosenlund, and Johansson (2000) promotes the public space shading, by advancing the concept of “shadow umbrella” for tropical climates. For Brandão (2004), this approach prevents taking advantage of the water heating and energy conversion. A proposal for guaranteeing a minimum solar access was developed by Duarte, Brandão, and Prata (2004) to promote the setback regulation for the Brazilian municipal building code.

The insertion of densification and verticalization strategies in the city is not a painless operation. The co-occurrence of new urban models and the existing neighborhood generates a new specific urban mix. Conversely, macro-planning actions, aiming to densify extensive portions of well-infrastructure-supplied urban land, are implemented before considering the specificities of each territory. In the São Paulo city Master Plan, for example, the development of Neighborhood Plans is subordinated to the densification along transport corridors (TOD). These plans foresees integrating the local road system within the mobility network, to promote social interaction by improving the quality of public spaces and green areas, as well as to value the cultural and environmental heritage (São Paulo Municipal Law, N° 16.050, of July 31, 2014). They aim to strengthen the Municipal planning system at the neighborhood scale.

Based on these contingencies, this paper aims to investigate the current morphological changes that affect contemporary Metropolises. A method of climate and morphological analysis at local scale was conceived. In order to accomplish the method proposed, a São Paulo neighborhood was selected as a case study; within the spatial arrangement of urban cross-sections, a field collection of environmental and morphological data is performed to calculate the proposed indicators. The climate variables, propitiated by such spatial arrangements, are considered key data for assessing the quality of spatial structures that the metropolitan cities progressively formalize. They could be used to evaluate the environmental sustainability of urban modifications when TOD strategies are implemented in the existing urban fabric.

2. Method for morphological-climate assessment in neighborhoods affected by land use change and densification processes

According to Chatzidimitriou and Yannas (2016), in most climate studies, the behavior of individual parameters is discussed separately, without a comparative assessment that could support the choice of the best suitable design options for a specific urban space. In order to elaborate a really useful urbanism tool, an integrated and comprehensive method has been drafted. Its aims is to perform a simplified neighborhood analysis that, besides giving a faithful depiction of the area, could be a support tool for decision making. Simplification is necessary to create an applicable protocol, useful to be implemented in the bureaucratic structure of city planning. The method is applicable in metropolis neighborhoods that change rapidly, often losing their qualities, for which it is critical to analyze the urban form variability and the resulting climate parameters at the micro-urban-scale.

2.1. Reference past experiences in neighborhoods assessment

Different research methods, in various geographical latitudes, have been developed to monitor the climate changes connected with the development of urban territories by way of expansion and land use transformation. According to Oke (2006), three scales of interest may be pursued to climatically analyze an urban fabric: the meso-scale, the local scale and the micro-scale. While the meso-scale phenomena influence the whole city, the local scale includes the climate of neighbourhoods with similar urban structures but excludes microclimate effects. The microscale, instead, analyzes building, open spaces, tree and street canyons; these objects have their own microclimate that

extends to the vicinity, too, causing close thermal differences even of numerous degrees (Oke, 2006). A micro-scale investigation is addressed by the method proposed herein. For the case of São Paulo, the three scales – meso, topo and micro – are reaffirmed by Tarifa and Armani (2000). For these authors, within the space of a topoclimatic unit, many microclimatic environments should be redefined. They consider the micro-scale a level of dwelling, living and working; it includes internal or external microclimatic environments in which alterations of atmospheric states have been proven.

This climatic fragmentation is caused by the external space design, as well as by the set of physical, biological, human and social interactions that come alive in these places; little local differences occur in temperature, wind flow and air pollution concentration (Duarte, 2010). For Aniello, Morgan, Busbey, and Newland (1995), these anomalies are micro-urban heat islands (MUHIs), “isolated urban locations that produce ‘hot spots’ within a city”, related to canyon geometry, material thermal properties and waste heat from buildings.

Joshi and Bhatt (2012) affirm that a constant observation of the land surface temperature variations is critical to recognize the formation of UHI at the early stage of Micro Urban Heat Island, which could be prevented by planning. Effat and Hassan (2014) show that asphalt and roof metal strongly contribute creating micro-urban heat islands in Cairo, especially in the absence of green and shadows. Wong et al. (2011) demonstrate that the urban form strongly affects the temperature at the micro level of locations; for the authors, UHI is a growing concern that has to be studied at all levels, from the macro to the micro level.

2.2. Method for analyzing the climate and morphological micro-scale of neighborhoods

This methodological proposal aims to climatically and morphologically characterize an exemplary site affected by densification and verticalization, in which a compact growth policy is fostered by city planners. The method was conceived and applied to a specific context of São Paulo, but is suitable to be replicated in other surrounding urban areas, other Brazilian cities and also abroad, under similar urbanization conditions and climate characteristics, in order to address future urban tissue modifications at the neighbour scale. The following flowchart (Fig. 1) describes the protocol to be followed for its application.

Firstly, a preliminary delimitation of the study urban domain, at the

neighbourhood scale, is required [Step (1) of Flow Chart]. Subsequently, the spatial structure has to be identified and characterized as a whole. Available geometric data – heights, land coverage, land use, built volumes, backsides – relative to each urban element, shall be collected from the available databases and integrated to field measurements [Step (2) of Flow Chart]. Next, the data will be analyzed to understand how these parameters are spatially distributed [Step (3) of Flow Chart]. Between Step (3) and (4), the first decision point takes place; at this moment, the suitable execution of the previous steps – domain selection, data collection and spatial analysis – should be verified. Afterwards, at [Step (4) of Flow Chart], to climatically explore the study area, representative study points have to be selected in the domain. Measurements should strive as much as possible to be simultaneous, analyze the measurement points variability in approximately the same weather conditions [Step (5) of Flow Chart]. Afterwards, the results of this fifth step have to be tabulated and processed for revealing the main micro-zones of climatic variations [Step (6) of Flow Chart]. Between Step (6) and (7), the second decision point takes place and the user has to verify if all the weather data have been accurately collected, in suitable weather conditions. According to Oke (2006), the best time to observe heat island effects occurs under calm airflow conditions and cloudless sky. To complement this climatic punctual analysis, the surrounding of the measured points should be morphologically analyzed, too. Additional geometric variables are measured in a suitable influence area around the climatic points analyzed [Step (7) of the Flow Chart] and a group of indicators is calculated [Step (8) of the Flow Chart]. Between Step (7) and (8), the last decision point takes place, in which the user has to confirm that the influence areas have been well characterized. Finally, to inspect the results, a comparison between the climatic analysis and the morphological characterization is performed [Step (9) of the Flow Chart].

2.3. Belenzinho case study, São Paulo

The Planalto Atlântico topography, in which the São Paulo Municipality is located, is characterized by the most varied forms, with peaks between 720 m and 850 m, about 45 km away from the Atlantic Ocean. A humid subtropical climate occurs in this region, characterized by a dry winter (from April to September), and a very rainy wet summer (from October to March) (Weather Station IAG-USP, 2016). Between 1961 and 1990, the annual average of minimum temperatures was

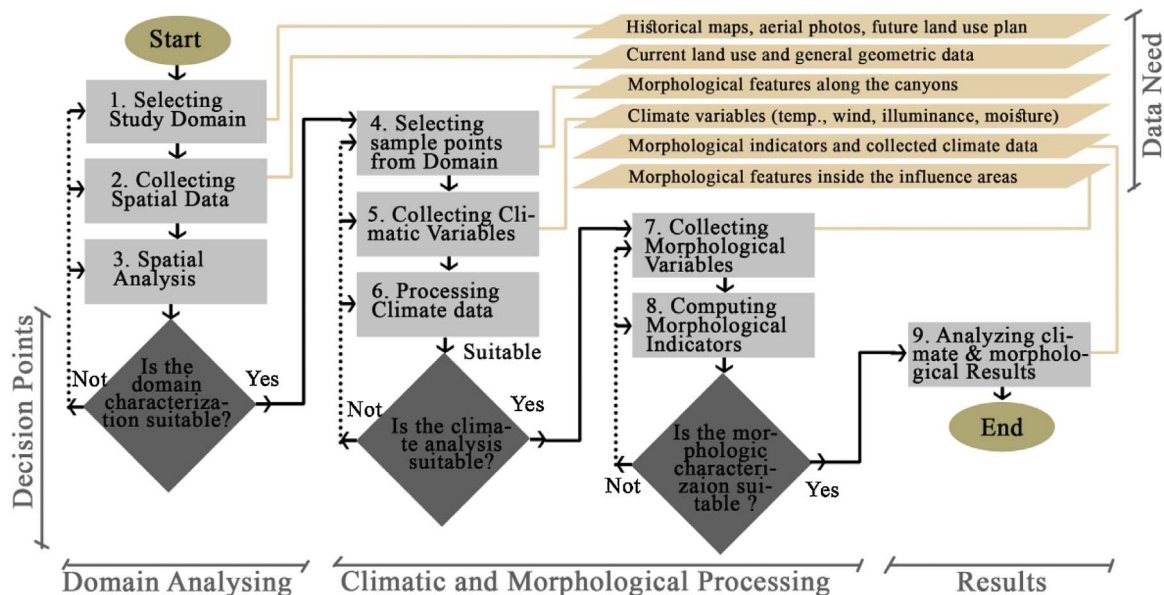


Fig. 1. Flow Chart. Source: Made by the Authors.

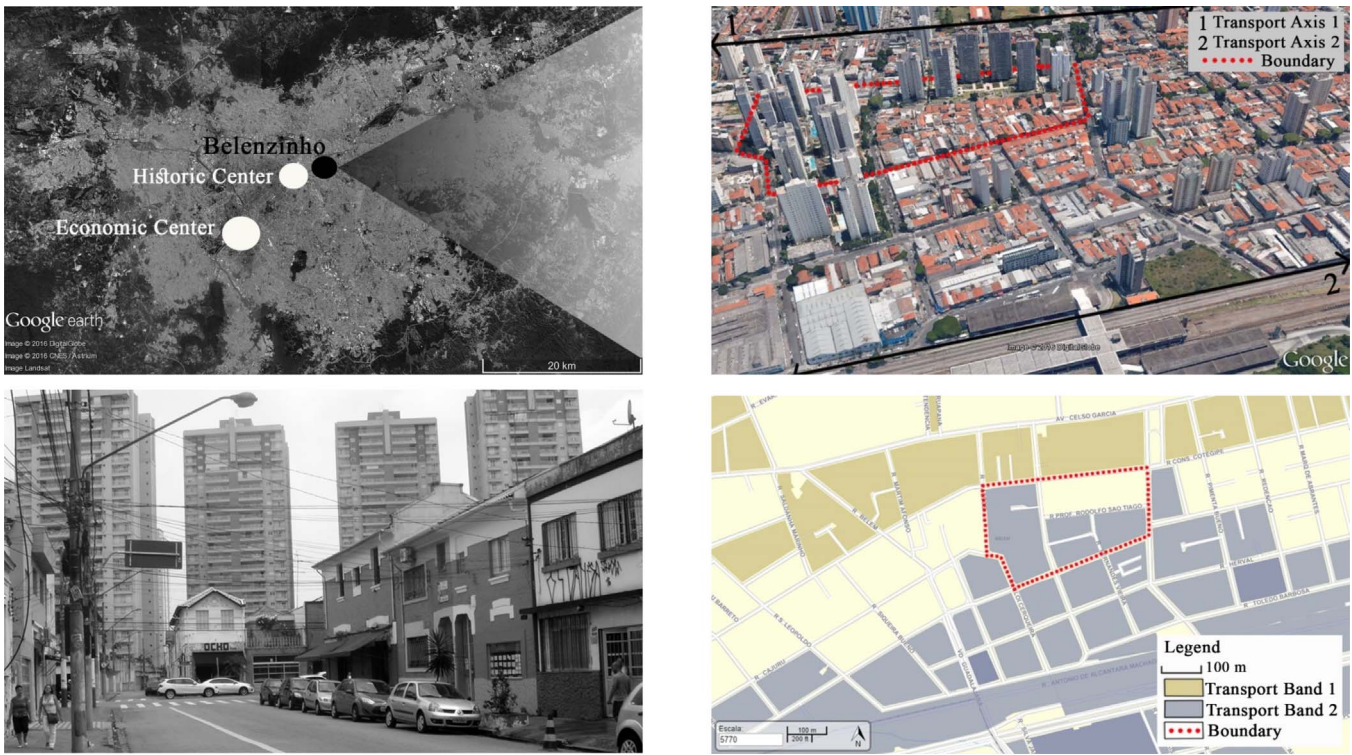


Fig. 2. Belenzinho Neighborhood (a), The Domain (b), Two coexisting fabrics (c), Land Use (d). Source: Google Earth (2016) (a), Google Earth (2016) (b), made by the Authors (c), made by the Authors, based on the Geosampa-Digital Map of São Paulo City, 2016 (d).

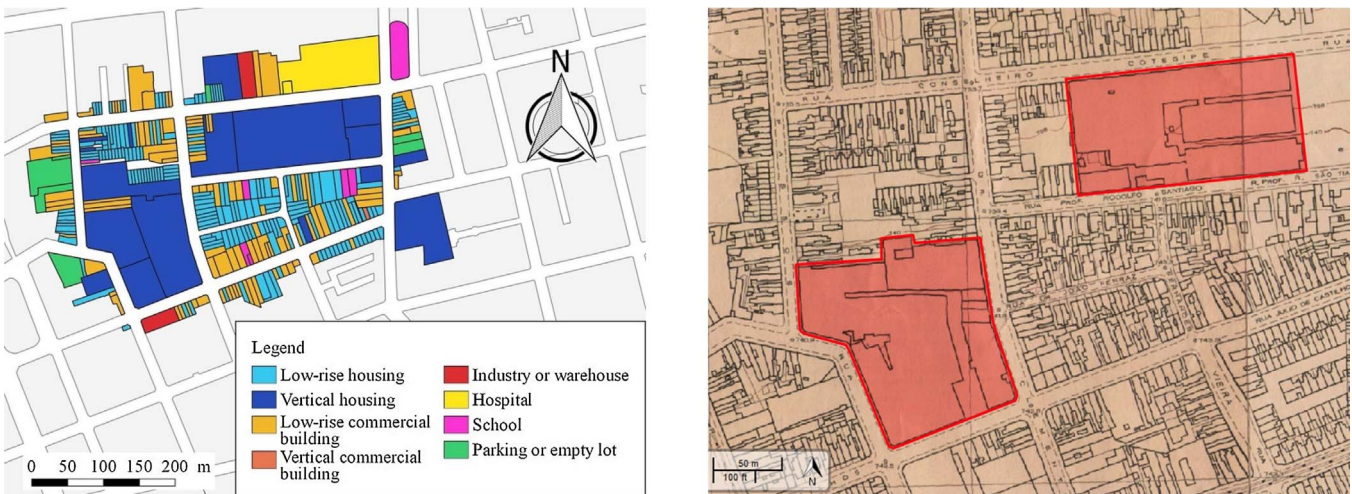


Fig. 3. Map of land use analysis (a). 1954 cadastral map of the study area (b). Source: Made by the Authors, based on the Geosampa-Digital Map of São Paulo City, 2016 (a). Vasp Cruzeiro, PMSP, 1954 (b).

15.5 °C (Tarifa & Armani, 2000).

The neighborhood of Belenzinho, located in the East zone of the city of São Paulo (Fig. 2a), is marked by flat terraces and wide hills (Tarifa & Armani, 2000). Inside this region, an urban study domain of 100 ha (Fig. 2b) was selected to apply the methodological proposal; the area is affected by people and built densification processes, according to the Land Use Policy of São Paulo (Municipality of São Paulo, 2014). The selected domain consists of five blocks, in which two different building typologies coexist, the oldest and newer grain (Fig. 2c), and is crossed by two important transport axes (Fig. 2d) [Step (1) of the Flow Chart].

Subsequently, the selected area was explored by means of field site visits, to verify the morphological features, the actual land use and the available metadata. In terms of urban morphology, the oldest grain is composed of compact low-rise fabric, organized in small lots with at

most three-story houses; conversely, the newer grain comprises open high-rise fabric, occupying large lots with towers and closed empty spaces around. The first fabric exhibits restricted road sections that slowdown cars and invites to walking; the geometry of verticalized fabric, instead, results in larger road section and receives different forms of mobility. Between these two categories, few other intermediate types can be found [Step (2) of Flow Chart].

3. Results of the method application to the Belenzinho neighborhood, São Paulo

According to the guidelines previously exposed, the present method assumes that the urban form variation leads to different climate environments and, consequently, to diverse conditions of livability and

comfort at the pedestrian scale. Therefore, a selected urban area was spatially analyzed, detecting all the possible configurations in which urban forms and open spaces are combined. Then, the climate and morphological state of these spatial configurations was assessed, showing thermal contrasts inside the domain.

3.1. Analyzing the spatial variability of the urban domain

To begin the Spatial Analysis ([Step (3) of Flow Chart]), an on-site land use investigation was performed in the selected area to confirm the foregoing observations. The land uses were segregated as shown in Fig. 3a. The study clearly reveals two coexisting fabrics previously identified as vertical housing lots, as well as low-rise housing and commercial lots. Fig. 3b presents a 1954 cadastral map of the study area, in which the lots formerly occupied by industries or warehouses are highlighted. Recently, with the receding industrial activity in the neighborhood, vertical housing has occupied these vast properties, while low-rise blocks of small lots still retain the original structure. Real estate developers, in fact, face difficulty in pooling several small lots and focus their action on areas with fewer larger lots. Therefore, since larger lots have already been developed within the studied area, the present configuration is expected to last for the next years. Under these contingencies, the TOD policy could not completely be carried out on-site. Despite this, a future external densification could be of interest to the surroundings, since some empty lots (including parking lots) and industries were identified on the border of the selected area. These lots might be developed in the coming years, causing further changes in the flow of mobility and the land value of the studied area.

The spatial analysis continues ranking the morphological distribution of the built and open spaces. Since the height is the main distinctive feature which detaches the differences between built form typologies, the urban fabric is subsequently classified by building vertical extension. Therefore, the buildings heights – available in the São Paulo Municipality database (Geosampa, 2016) – were classified in four vertical scales. Since the heights generally allow a certain number of built floors, the scales also provide an approximate value of the land use intensity. The first scale gathers the unbuilt spaces, paved or permeable, while the others segregate the built areas. As the scales are associated with the urban elements, one lot might contain more than one scale: Scale S1 = 0 floor, (0 m < S1 ≤ 0.5 m); Scale S2 = 1–3 floors, (0.5 m < S2 ≤ 10 m); Scale S3 = 4–9 floors, (10 m < S3 ≤ 30 m); Scale S4 = > 10 floors, (S4 > 30 m).

Then, the scale spatial distribution was valued with regard to four categories: the number of buildings (1), heights (2), areas (3) and volumes (4). In each of the four graphs, the scale impact can be observed; Fig. 4(a) shows Scale S2 is the most widespread, gathering the great majority of built elements present in the study area, followed by S4; just few elements of S3 and S1 were found, since the lots do not have many open spaces (S1) or intermediate-scale buildings (S3). Despite this scale disparity, in Fig. 4(b), Scale S4 reaches S2, or rather the amount of meters measured in height is roughly the same between the two scales (1400 m versus 1200 m of linear development). This means that the two scales approximately provide the same number of inhabited floors, despite their different footprint, once scale S4 benefits from the

verticalization potential. Scale S1 shows a rising behavior only in Fig. 4(c), where the large tower podiums (around 0.1 m–0.5 m of paved built thickness emerging from the ground level) significantly influence the amount of constructed area. The final overcoming of Scale (4) with respect to Scale (2) occurs in Fig. 4(d), wherein the built volume amount is calculated for each scale. In general, it may be clearly observed that the scales are not equally and gradually distributed.

A gap between the largest (S4) and smallest (S1 and S2) scales was found; the near absence of intermediate scales (S3), in fact, is noticed. This result is in agreement with Salingar and West findings (1999), for whom the largest amount of money supply is currently addressed to finance giant projects, to the detriment of small and intermediate size projects that, instead, could favor an organic growth of the building fabric. The four graphs constitute a simple tool of morphological assessment, obtained from easily available data. They allow investigating the reciprocal influences between the number of built elements, heights, areas and volumes in each scale. Fig. 5a displays the built forms ranging inside the red perimeter of domain and surroundings. Very verticalized blocks (burgundy) and other lower built blocks (orange shades) were found juxtaposed at very close distances, contributing to the scattering of the urban fabric. At this stage of the flowchart (Step 3), the accuracy of the collected data was checked.

3.2. Selection of representative points of the domain according to climate and the urban form criteria

By using Table 1, the thirty-six representative street cross-sections were selected inside the domain (Fig. 5b) as instances of different spatial situations to be analyzed [Step (4) of Flow Chart]. Five descriptive categories – Vertical Scale (1), Retreat (2), Street Orientation (3), Type Street (4), and Placement (5) – were identified. Each category is split into classes; the classes take into account the variability of the category along the canyons and allow distinguishing one urban section from the others. Each road section is made up by the street open space flanked by two built elements on both sides (Fig. 8b). The street geographical orientation is taken into account owing to its influence on natural ventilation and surface temperatures. Because of its singularity, each section differs from the others by one or more of these morphological properties. The thirty-six samples represent a wide range of climate conditions a pedestrian may experience by walking across the neighborhood open spaces, testing different comfort environments. In fact, for Oke (1987), on the canopy layer, the air performance is related to the type of canyons and the distance between buildings. In each urban section, a point of measurement was identified for the climate assessment (Fig. 5b). The points are located in the public spaces, because the entrance to most of the blocks is closed with gratings. Furthermore, the points are just a little retreated from the crossroads, so as to avoid interferences with other street axes.

3.3. Climate assessment

In Steps [5 and 6 of Flow Chart], a transect path was traced through the thirty-six points, to explore the microclimate environments that make up the urban domain, under autumnal and winter meteorological

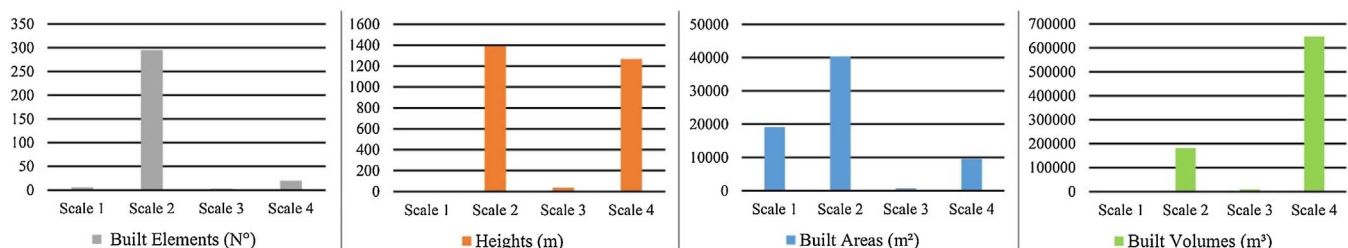


Fig. 4. Built Elements (a), Heights (b), Built Areas (c), Built Volumes (d).

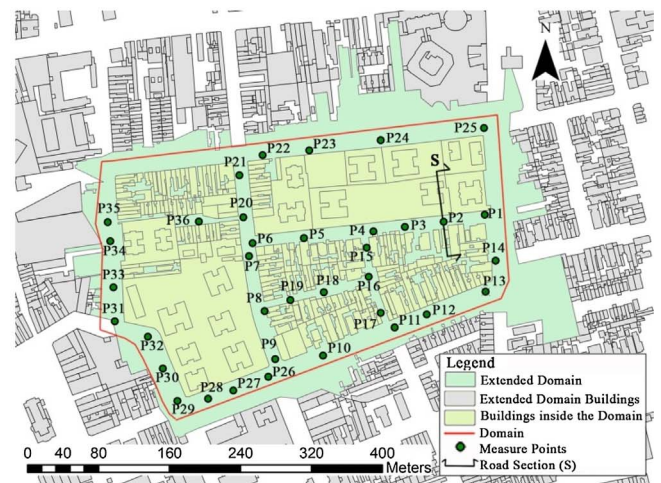
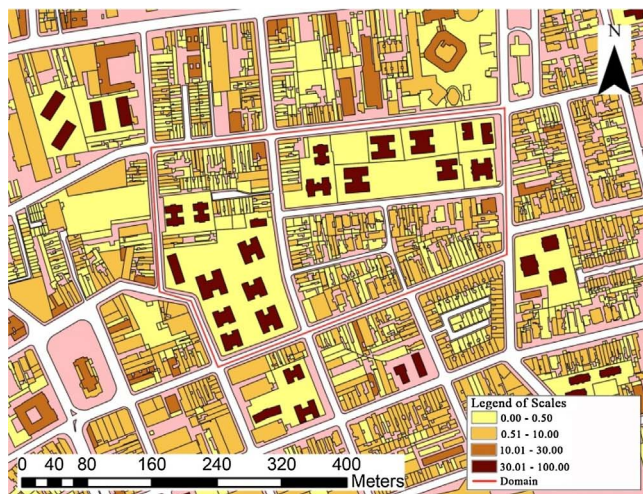


Fig. 5. Ranging of scales inside the study area (a). The measure points within the larger domain (b). Source: Made by the Authors, based on the Geosampa-Digital Map of São Paulo City, 2016 (a & b).

conditions. The collection points were placed in the same relief conditions, on the sidewalk, space of morphologic binding and meeting between urban forms. The equipment is thus protected from the cars movement and is accessible by operators. The equipment used includes: Datalogger: Hobo, U23-001; Solar shield: Hobo, RS-1 (to measure air temperature and moisture); Hot wire anemometer: Testo, 425 (to measure wind); Digital luximeter: Homis, 630 (to measure illuminance); Thermographic camera: Fluke, Ti105 (to measure surface temperature), Photographic camera: Nikon, Coolpix 4500; Fisheye lens: Nikon, FC-E8 0.21x (to measure sky view); Electronic tape: Leica, DISTO D810 touch (to measure geometry).

In order to assess the climate variations under approximately simultaneous atmospheric conditions, the measure time between the sample points was minimized to 15 min; this is the time required for the HOBO equipment to stabilize (5–10 min), for the hand measurements,

plus the time required to move the equipment from one point to the next (3–5 min). It was thus possible to measure 12 points a day twice, in the morning (6:00 a.m.–9:00 a.m.) and along the afternoon (13:00 a.m.–16:00 a.m.). These temporal ranges were chosen by detaching the colder and the warmer periods that mark the daily temperature trend during the cold season. In fact, according to Oke (2006), to reveal the thermal and moisture anomalies, the collection period has to be chosen by maximizing the micro-climate differences. The weather bulletins of the nearest fixed meteorological stations – IAG USP (WMO: 83004, LAT: –23.65, LONG: –46.62) and CETESB Marg. Tietê Ponte dos Remédios (LAT: –23.52, LONG: –46.73) – were taken as a reference (Weather Station IAG-USP, 2016; Weather Station CETESB, 2017). In the case of the morning period, the band 5:00–6:00, albeit suitable to intercept the lows, was discarded to protect the equipment and operators from nocturnal criminality; hence, no measurement was made before 6:00

Table 1
Characterization of Domain in Categories and Classes.

Categories	Sketch	Description	Classes	Measured Points
Built Space	Vertical Scales on both sides	Each road section is bordered by a pair of buildings, on the right and left side. The building heights belong to one of the 4 scales.	$0.0 < S1 > 0.5$ $0.5 < S2 > 10.0$ $10.0 < S3 > 30.0$ $30.0 < S4 > 100.0$	6,14,25,27,34,35 2-22,24,26,28,29,31,33,35,36 10,13,21-23,27,32 1-5,7-9,23,25,26,28-32,34
Empty Space	Retreat	Each road section is bordered by a pair of buildings, on the right and left side. The building retreats belong to one of the 4 scales.	$R = 0.0$ $0.0 < R \leq 5.0$ $5.0 < R \leq 10.0$ $R > 10.0$	6-15,17,20-22,24,26-29,31-33,35,36 1,3-5,15,16,18,19,23-25,28 1,2,5,9,26,30,32,34 2-4,6-8,14,23,25,27,29-31,34,35
Street Orientation	North-South, East-West	The street in which the urban sections are traced can have one of three orientations.	North-South East-West	4, 6-9,12,14-17,20,21,29-35 1-7,10-13,18,19,22-28
Type Street	Main/Secondary	The street in which the urban sections are traced can be main or secondary; the first one receives a greater traffic volume than the second one.	Main street: $St < 12.5$ Secondary street: $St > 12.5$	6-14,20-35 1-7,12,15-19,36
Placement	Perimeter/Block	The urban sections take place in different locations of the Domain (inside or on the boundary) and of the blocks (inside or along the street).	Along the perimeter Inside the perimeter Inside the block Outside the block	10-14, 22-35 1-9,15-21,36 36 1-35

Table 2
Organization of field work – Execution Sequence for simultaneous measurements in field.

Intervals	15 min		
	5 min	3 min	7 min
Hobo Equipment	transport		stabilization and automatic measurement
Other Equipments	transport		manual measurement by operators
Operator 1	- go from one point to the next	- measures the surface temperatures - takes sky view photos	- places and calibrates the tripod - measures the street length, sidewalk length, retreat length, building height, by electric tape on the tripod - measures the intensity and direction of wind* - measures the illuminance* * one measurement per minute (7 times)
Operator 2		- notes the sky condition, shading, tree coverage, equipment location	

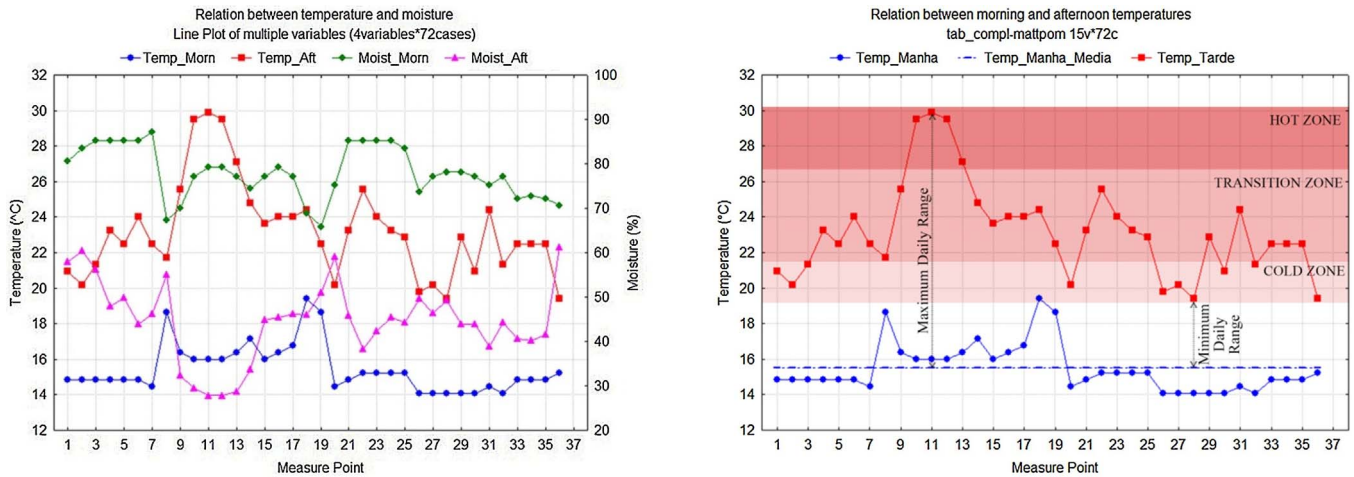


Fig. 6. Average morning and afternoon temperatures, average morning and afternoon moistures (a). Three climatic zones (b).

a.m.

Seventy-two hours (three days) were necessary to complete the measurement of the study area by two operators. The entire measurement cycle was repeated twice, once in the autumn and the other in the winter. In the first test, because of bad weather conditions, the three days were not consecutive (4, 25, and 26 of May 2016). In the second case, the progression was respected (12, 13, 14, and 15 of July 2016). Table 2 summarizes the organization of tasks which guided the field measurements.

Fig. 6a shows the course of the average moisture and air temperature. In the latter, the morning temperatures are approximately constant, placed around the average value of $T_a = 15.5^\circ\text{C}$, with only points P8, P18, P19 emerging above the general tendency, confirming the aforementioned average value found by Tarifa and Armani (2000). This trend is a common base, given by the night cooling, from which the city begins gaining daily heat. Consequently, in the afternoon, a larger variation may be observed, to the extent that each of the morphological groups overheats with different intensities. Therefore, the afternoon temperature trend is split into three bands – hot (1), transition (2) and cold (3) zone – in which the measured points can be segregated (Fig. 6b).

To measure the superficial temperature, a thermographic camera (Operator 1) was used. A specific emissivity was set before measuring each material. These emissivity values were obtained from Oke (1987); in the case of asphalt, an experimental measurement of the emissivity was performed on a sample of the material, made available by the Paving Technology Laboratory of the Transport Engineering Department (LTP) of USP. The resulting value (0.96) was adopted in the field.

The measurements were taken at three points of each cross-section: the street pavement, the sidewalk pavement and the building façade wall adjacent to the sidewalk. In Fig. 7a, the results of superficial and air temperature were overlapped with those relating to the illuminance

level, in the morning and afternoon periods.

The average correlation between surface temperatures and illuminance was computed at all the points by Spearman's Rank-Order Correlation (Fig. 7b). From the scatter plot (Fig. 8a), it may be seen that the three surface temperatures have almost parallel regression lines and are therefore related to the illuminance on a similar way. A threshold in the correlation distribution could be verified, denoting a data bilinear behavior. Subsequently, the Sky View Factor (SVF) was chosen as split parameter to cluster the data population in two groups (high SVF, low SVF). SVF was obtained by using the software Rayman 1.2. 25% was considered as the SVF cut-off value. By repeating the correlation in these two groups, the correlation of high SVF group was observed to increase when compared to the average results, whereas the low SVF group decreased strongly. As expected, among other factors, a wide sky view enhances the correlation between illuminance and temperature, while the presence of obstructing objects disturbs it.

Finally, the presence of tree coverage was also observed. Three classes of urban tree coverage were qualitatively detected in the study area at the 36 points: (i) no tree coverage, (ii) low tree coverage, (iii) high tree coverage. Fig. 8c visualizes how street tree coverage contributes to mitigating the local micro-climate by decreasing hot temperatures; points with green bins have lower temperatures than points without green bins. Along the temperature line (dashed line), five sets of points were highlighted (continuous line). Each set is formed by points in similar local conditions – same street, same street orientation, similar built surrounding, at really close distance. It can be observed that, in these sets, high tree coverage is largely responsible for the temperature drop.

3.4. Morphological assessment

In order to understand the implication of the urban form for the

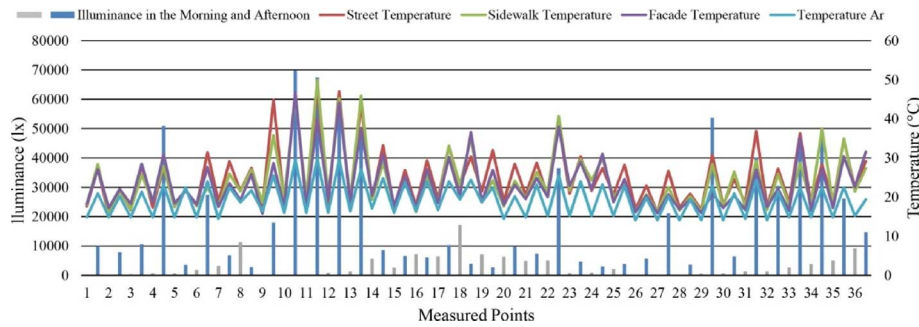


Fig. 7. Illuminance and Temperature in the morning and afternoon (a). Spearman Rank Order Correlation (b).

Surface Temperature	Illuminance		
	All Points	High SVF	Low SVF
Street	0.771	0.822	0.581
Sidewalk	0.705	0.755	0.509
Facade	0.661	0.739	0.377

*Significant correlation at $p < 0.05$

**Cut-off value between High and Low SVF = 25%

climatic data gaps, the influence area around the measured points is traced and explored in greater detail [Step (7) of the Flow Chart], by collecting the main morphological features inside it (Fig. 9). Different references were consulted to choose the most proper size for the influence areas.

According to Oke (2006), for the temperature and humidity sensors, the influence circle varies with the building density around a radius of 0.5 km. Instead, when the sensors acquire the signals via turbulent transport, the source area is an elliptical shape, aligned in the upwind direction. For Grimmond (2006), also the measurement method, the equipment location, the surface on which it is positioned, the weather conditions, the research objective and the type of climatic variables measured are significant issues that should be considered in the choice of the influence area.

In the case of this article, because of the abundance of climatic variables analyzed, distinct influences areas should have been established. Therefore, in order to evaluate the built space effect on the ensemble of the variables analyzed, the influence area adopted amounts to a circle of 40 m of radius, centered in the measuring point (Fig. 9). The width of this area considers the necessary range to cover the maximum width of the urban sections under consideration. Since the buildings that surround the points on the perimeter exceed the boundary of the red Domain, a larger area of Domain (in green) will be taken into account to conduct this step (Fig. 5b).

In order to analyze these new data inputs, [Step (8) of the Flow Chart] computes six types of indicators in each sample. The Indicators of Intensity, Diversity and Compacity take up the proposal for Indicators of Bourdic, Salat, and Nowacki, (2012), while the Indicator of Frequency is based on the ideas of Multiplicity expressed by

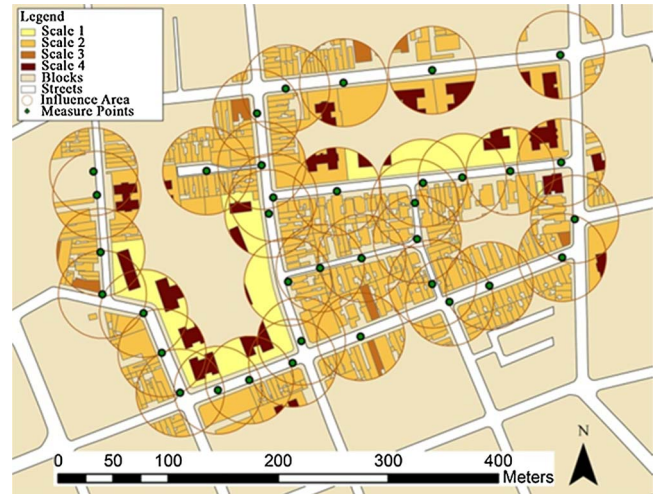


Fig. 9. Influence areas of measure points.

Source: Made by the Authors, based on the Geosampa-Digital Map of São Paulo City, 2016.

Salinger and West (1999). However, all the indicators were adapted to the specific framework of the Method and to the neighborhood scale, besides proposing the built and open spaces as new reference measures for the urban form assessment. The computation of Indicators is shown in Table 3.

Indicators are key instruments, designed to complement the climate results; they are expressed in percentages or numeric quantity and

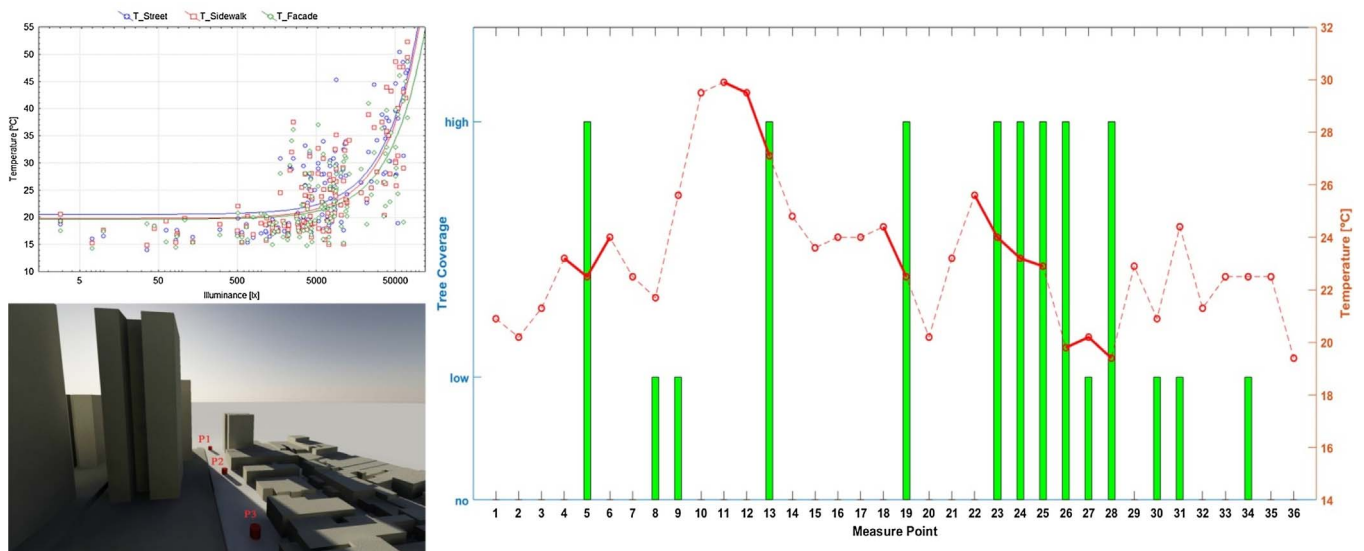


Fig. 8. Surface Temperatures and Illuminance Scatter Plot (a). 3D representation of an urban section S at points P1–P3, at 7:30 a.m. (b). Air Temperature and Tree Coverage (c).

Table 3
Indicators.

(1) Indicators of Coverage:

Empty Area (%) = $100 * \left[\left(\sum_1^n \text{Sample Empty Area} \right) / \text{Sample Area} \right]$ with $n = \text{number of empty areas}$

Built Area (%) = $100 * \left[\left(\sum_1^n \text{Sample Built Area} \right) / \text{Sample Area} \right]$ with $n = \text{number of built elements}$

(2) Indicators of Intensity:

Void Volume (%) = 100% – Built Volume

Built Volume (%) = $100 * \left[\left(\sum_1^n \text{Sample Built Volume} \right) / \text{Ideal Volume} \right]$ with $n = \text{number of built elements}$
with $\text{Ideal Volume (m}^3\text{)} = \text{Sample Area} * \text{Built Element Average Height} = 100\%$

(3) Indicators of Frequency:

Built Elements Frequency (n°) = $\sum_1^n \text{Built Element}$ with $n = \text{number of built elements}$

Voids Frequency (n°) = $\sum_1^V \text{Bounded Void}$ with $n = \text{number of bounded voids}$

(4) Indicator of Compacity:

Built Elements Proximity (n°) = $\sum_1^n \text{Wall shared by more Built Elements}$ with $n = \text{number of built elements}$

(5) Indicators of Permeability:

Openings Areas (%) = $100 * \left[\left(\sum_1^n \text{Openings Length} \right) / \text{Lot Perimeter} \right]$ with $n = \text{number of lots}$

(6) Indicator of Diversity:

Vertical Diversity (n°) = $\sum_1^n \text{Scale}$ with $n = \text{number of built elements}$

Horizontal Diversity (n°) = $\sum_1^n \text{Retreat}$ with $n = \text{number of built elements}$

computed with regard to the influence area. The proposal of their use enhances the method structure, conferring originality. The Indicators of Coverage (1) show how the area around the point of measurement is covered by buildings or if it is free of them. The higher value was found at point P36, the only one located inside the block; the lower, instead, occurs close to a group of towers (P25). Fig. 10a shows that, overall, the built area surpasses the empty (or open) area, although the latter also includes the footprint of streets. The Indicators of Intensity (2) display how this occupancy is heavily or slightly built, by computing the constructed volume of buildings. Conversely, the void volume was obtained by subtracting the built volume percentage from the ideal volume related to the influence area (100%). The ideal volume has the influence area as a base and the average height of the domain as the vertical extension. The highest value was found at point P24, which includes two towers in its area; the lowest occurs close to a large private vacuum created by a condominium (P4) (Fig. 10b).

The results demonstrate that built element frequency and compacity perform the same path; by increasing the number of built elements, the compacity of urban fabric rises, since the proximity of built elements

increases, too. Besides, a similar trend is exhibited by the Indicators of Diversity that measure the degree of landscape morphological diversification; as the number of detected scales grows, the number of retreat types also rises (Fig. 11a). Finally, in Fig. 11b, the inverse relationship between the lot permeability and the frequency of voids is presented; as the first indicator increases, revealing the continuity between the street open spaces and the empty areas inside the lots, the degree of space fragmentation of urban fabric (high number of voids) follows the reverse path. This means that, the more a lot presents permeability of its boundaries, the more the lot exhibits a low multiplicity of open areas within it.

4. Discussion: overall comparative assessment of results and indicators

A comparative analysis between the two types of results is crucial to carry out [Step (9) of the Flow Chart]. The first important observation suggests that, despite the small size of the domain, climate variability was measured between the points; a strong correlation between environmental patterns and morphological structures of the studied area was observed. These results agree with Stewart, Oke, and Krayenhoff (2014), for whom building height and spacing between buildings contribute to creating thermal contrasts among different localities, along with tree density, soil wetness and permeability. The occurrence of thermal contrasts results in various climate zones in which the open space comfort changes slightly.

Three climatic zones were identified: Hot Zones (1), Transition Zones (2) and Cold Zones (3). While transition zones present intermediate temperatures, cold and hot zones show temperature peaks. Therefore, it can be inferred that, in the cold season, the former provide more suitable open space for staying and favor the pedestrian circulation, countering the motor vehicle transit that causes atmospheric pollution harmful to human health; regarding the second, instead, urban improvements should be thought to restore a friendly and well-connected pedestrian network. Each point of domain falls on one of three zones, in accordance with the collected afternoon temperature. Fig. 12 shows how these climatic zones are distributed inside the domain, grouped into sets of points.

4.1. HOT ZONE: Uncovered Spaces in low-rise fabric (P10, P11, P12, P13)

The “hot zone” is the region in which the domain presents the highest heating. Here, starting from a pretty constant morning level, points P10, P11, P12, and P13 together reached the highest afternoon temperature, exhibiting the larger thermal excursion (13.50 °C, 13.90 °C, 13.30 °C and 10.70 °C). Conversely, the lowest values of moisture were found in the morning period. In addition, the highest values of surface temperature were found in correspondence with the street, sidewalk and façade of the same points.

This exceptional trend is performed by four street cross-sections, placed in sequence along the same canyon (Fig. 13). These source

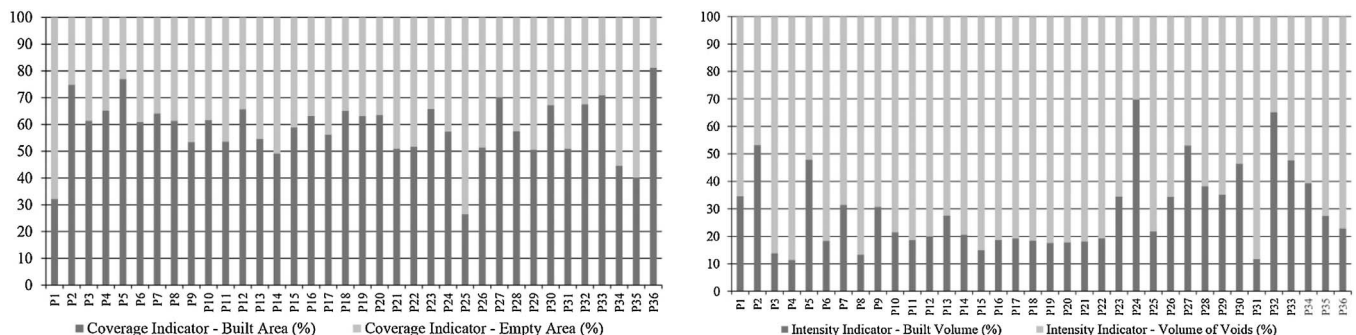


Fig. 10. Built Area and Empty Area (a), Built Volume and Void Volume (b).

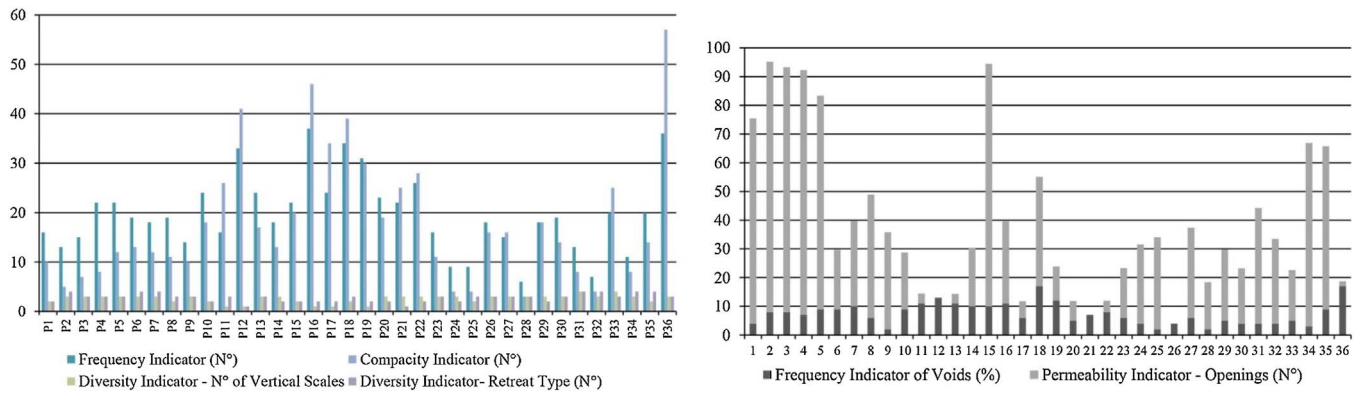


Fig. 11. Frequency of elements, Compacity of built mass, Diversity of scales and retreats (a), Frequency and Permeability of Voids (b).

points are characterized by unshaded open spaces, free from architectural obstructions. The main block of towers is quite far. In addition, as the building heights in these points are modest, the proximity of houses to the sidewalks does not prevent solar access, as the sky views show (Fig. 12). Therefore, the sun path – following the arc East-North-West, permits a full radiation of the road sections, their exposed materials, as well as of the building roofs, causing high levels of outdoor temperatures.

From the morphological analysis of the “hot” spatial situations, a small amount of built volume (21%, 19% and 20%) was measured at points 10, 11, 12, implying high percentages of void volumes which mean open air spaces. Also, low diversity (20%, 3% and 0%) and low permeability were found. At points 11 and 12, in fact, just scale S2 is present (0.50 m < S2 < 10 m), precluding the presence of buildings with different heights, which would favor ventilation. Few or no openings cross the lot boundary, also preventing any cooling action exercised by secondary air streams. In addition, at point 12, just one type of retreat was observed (R = 0), and the perimeter of the lot directly faces the street.

4.2. COLD ZONE: Shaded Spaces (P1, P2, P3 and P26, P27, P28)

The “cold zone” includes the coolest regions of the domain. In this range, two groups of contiguous urban sections – P1–P3 (set 1) and P26–P28 (set 2) – perform the “lows” in the afternoon temperature line (between 19 °C and 21 °C) with small thermal excursions in the morning constant temperature. Both of these sets are characterized by open spaces widely shaded by towers on the north side; this prevents a

direct irradiation on the south side and slows down the daily heating process.

Points P1–P3 are located between a group of towers on the north flank and a fabric of low-rise housing on the south one. The shading towers are arranged in two distinct lines of the lot; one facing the street, and the other at the back of the plot. This shifting creates a dense urban arrangement that permanently or temporarily cast shadows on the points below (Fig. 13a and b). According to Knowles and Berry (1980), the larger the built volumes, the more the buildings conflict with each other by shadowing. Thus, when the measured points are intercepted by more towers (P2), the temperature tends to fall, since the points are longer shaded.

On the same street, along with hot spots – Rua Júlio de Castilhos –, the second set of cold points were pinpointed (P26–P28). Between the hottest and coldest regions on this street, an excursion of 9.7 °C was measured. Here, besides the shading caused by the high-rise buildings, an additional sun cover is exercised by trees. The tree coverage contributes to additional cooling effects. While a fall of afternoon daylighting was observed from P27 (low coverage) to P26 and P28 (high coverage), a surface temperature decrease was verified, especially in the case of the road asphalt (20.8 °C (P26), 25.0 °C (P27) and 19.1 °C (P28)). Consequently, despite the small distance between the points, an air temperature excursion occurs between P26 (19.8 °C), P27 (20.2 °C) and P28 (19.4 °C).

The urban form that characterizes the cold zone can be understood by analyzing the morphology of cooler points surroundings. Primarily, these points are composed of a variety of different scales and retreats, since different building typologies are found within a walking distance.

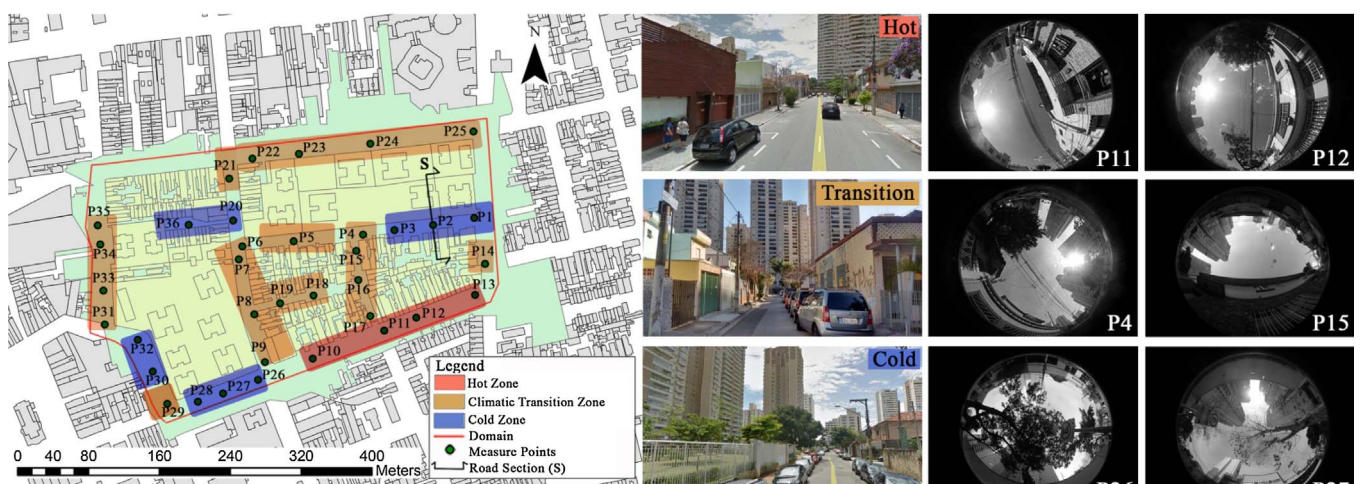


Fig. 12. Map of climatic zones (left, a), representative pictures of the three zones (center, b), sky view photos (right, c). Source: Made by the Authors, based on Geosampa-Digital Map of São Paulo City, 2016 (a). Made by the Authors (b & c).

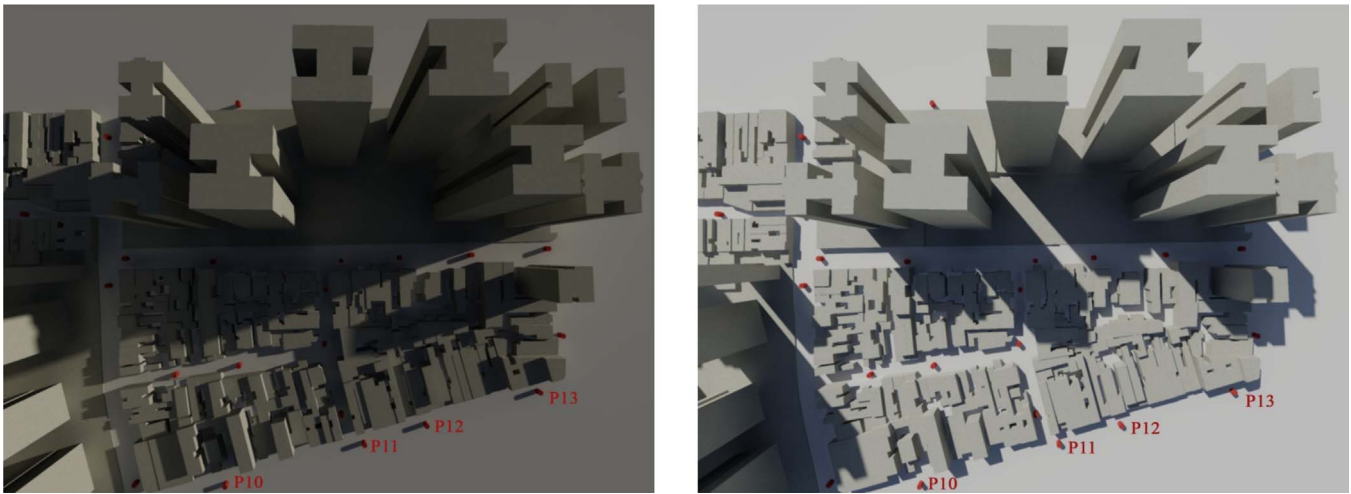


Fig. 13. 3-Dimensional domain representation at 7:30 a.m. (a) and at 2:30 p.m. (b) showing the points P10–P13 constantly lighted.

All of them include towers, ensuring an abundance of retreat types and the presence of the major scale S4. In the case of the P2 influence area, for example, four retreat types were found. Instead, different values of lot permeability were computed between the two sets of points. While the first set (P1–P3) has high values (71%, 87%, 85%) due to the absence of walls along the block perimeter, the second one (P26–P28) has quite closed boundaries and, consequently, low values of openings (0%, 31%, 16%); hence, air dynamics differently affect pedestrians' walk in these two zones. According to Emmanuel et al. (2007), shading strategies should be coupled with a street level ventilation study at building and neighborhood scale.

4.3. TRANSITION ZONE: Internal and Protected Spaces (P4, P15, P16, P17)

Moving away from the uncovered urban fabrics, the “hot zone” fades, as well as leaving the shaded open spaces, the effects of “cold” zones dissolve. Between the “hot” and “cold” zones, transition regions take place. In the case of the study domain, the zones of climatic transition are rather scattered. However, similarities could be identified between points P4, P15, P16, P17. This group of four points runs approximately along the North-South direction, between the “hot” and the “cold” zone; their benefit from partial shading and slight ventilation was registered along their axis. To the North of point P4 (Fig. 12), a large square provides an open space that favors more radiation and avoids the direct shading of the towers. Because of this opening, P4 receives a good afternoon level of illuminance and multidirectional ventilation, both parallel to the street. Conforming to the air trend, the surface temperatures achieve intermediate values in this zone (Fig. 7).

From a morphological standpoint, other considerations could be extracted. The surroundings of these transition zone points show a quite balanced coverage proportion between the built and void areas (65–35%, 59–41%, 63–37% and 56–44%). Concurrently, the small built volume percentages (11%, 15%, 19% and 19%) turn out a modest compactness and verticalization in these influence areas. The built volume percentage around point P4 is the smallest. In addition, since the transition zone corresponds to a historical fabric, a high frequency of built elements occurs, especially in the influence area of point P16, in which the major value was found (37%).

In the same line of P1, P2, P3, sample P6, located on the corner, stands out from the previous cold spots, exhibiting warmer transitional temperature (24.0 °C). In fact, despite being skirted by towers, it leaves the morning shadowing area before the other points, benefiting from the afternoon sun. This circumstance comes from the physical arrangement around the point; in fact, from P1 to P6, the towers fade

from a height of 73 to 59 m, before disappearing near the lot corner, in which a playground is located.

5. Conclusion

The method focused on the study of urban fabrics at the local scale, affected by densification and verticalization, correlating the spatial arrangement of urban cross-sections and the related micro-climate conditions. A new approach is proposed with regard to the combined study of urban form and climate, focusing on the microscale in which the pedestrian comfort varies significantly. In practical terms, the method could be applied to assess the comfort of urban spatial arrangements when built modifications are implemented by the TOD strategies; it contributes to enhancing the dialogue between decision makers, planners and researchers.

The methodology is intended to be replicable for tropical climates in which south-world metropolitan areas grow under the impetus of exploitative real estate forces and unstable governments. The flowchart proposed aims to provide a guiding tool apt to favor its repeatability. In addition, the method application grants results that could support municipal planners involved in the conception of neighborhood plans, as well as in larger scale TOD strategies. Future improvements in the method structure could be addressed: (1) to enlarge the domain, in order to deal with a larger number of climatic environments, (2) to further the morphological analysis, exploring its climate performance, (3) to simulate future scenarios, comparing different urban design solutions.

According to the results, thermal contrasts have been found between the domain points. Three climate zones were identified, distributed in the assessed urban area, in accordance with distinct morphological patterns. The hot zone (1) was found in correspondence of low-rise urban fabrics, composed of asphaltic or metal materials, distant from vertical buildings, with a sky view free from obstacles, and without opening or retreats along the lots boundaries. Cold zones (3), instead, occurred within shaded open spaces, dominated by high-rise fabrics, below the tree canopy, as well as in internal open spaces, surrounded by horizontal compact fabrics and covered by material with lower thermal conductivity (P36). Finally, transition zones (2) were found in the middle of the hot and the cold zones, characterized by intermittent shading, scattered trees, buildings with different retreats and heights.

The climatic zoning shows the current micro-climate conditions of a São Paulo neighborhood in the cold season. Future land use changes and TOD urban interventions could soften or sharpen the intra-urban thermal differences recorded. In the case of the hot zone, the insertion

of a green corridor could moderate the highest temperatures; conversely, the further verticalization of the central blocks could result in a substantial temperature drop, because of shadowing. The treatment of cold zones, instead, is much more limited; the sun obstruction caused by towers is not easily reversible, and far more attention should be devoted to monitoring the insertions of additional built interventions.

In this way, the method also contributed to assessing the current open space quality of a São Paulo neighborhood, qualitatively understanding which urban interventions could still be planned to promote a pedestrian-friendly urban design, enhancing the open space experience, decreasing the traffic congestion and mitigating the local car-based pollution. In this sense, the method constitutes a critical urban design tool, able to guide future urban transformations starting from existing open space assessment.

Funding sources

This work was supported by the EACEA – Erasmus Mundus Programme, Action 2 – STRAND 1, Lot 16, Brazil; by the State of São Paulo Research Foundation – FAPESP (2015/10759-0) and by the Coordination for the Improvement of Higher Education Personnel – CAPES (2017).

Acknowledgements

The authors would like to express their gratitude to the Laboratory of Environmental Comfort and Energy Efficiency (LABAUT) of the Faculty of Architecture and Urbanism (FAU) of the São Paulo University (USP), to the Paving Technology Laboratory (LTP) of the *Escola Politécnica* (EP) of USP and to Professor E. S. Da Fonseca Junior, of the USP Transport Engineering Department, for the support in providing measurement equipment and samples.

References

- Aniello, C., Morgan, K., Busbey, A., & Newland, L. (1995). Mapping micro-urban heat islands using Landsat TM and a GIS. *Computers & Geoscience*, 21(8), 965–969.
- Barau, A. S., Maconachie, R., Ludin, A. N. M., & Abdulhamid, A. (2014). Urban morphology dynamics and environmental change in Kano, Nigeria. *Land Use Policy*, 42, 307–317.
- Bourdic, L., Salat, S., & Nowacki, C. (2012). Assessing cities: A new system of cross-scale spatial indicators. *Building Research & Information*, 40, 592–605.
- Brandão, R. S. (2004). *Acesso ao sol e à luz natural: avaliação do impacto de novas edificações no desempenho térmico, luminoso e energético do seu entorno. [Master Thesis]*. São Paulo: University of São Paulo. Accessed 07 September, 2016 http://www.fau.usp.br/aut5823/Acesso_ao_Sol/Me_2004.pdf.
- Chatzidimitriou, A., & Yannas, S. (2016). Microclimate design for open spaces: Ranking urban design effects on pedestrian thermal comfort in summer. *Sustainable Cities and Society*, 26, 27–47.
- Cheng, V., Steemers, K., Montavon, M., & Compagnon, R. (2006). Urban form, density and solar potential. *Proceedings of PLEA 2006 – The 23rd conference on passive and low energy architecture* (pp. 701–706).
- Duarte, D., Brandão, R., & Prata, A. (2004). Environmental criteria incorporation in a Brazilian Building Code. *Proceedings of Plea 2004 – The 21th conference on passive and low energy architecture*.
- Duarte, D. H. S. (2010). Variáveis urbanísticas e microclimas urbanos-modelo empírico e proposta de um indicador. *Fórum Patrimônio: Ambiente Construído e Patrimônio Sustentável*, 3(2).
- Effat, H. A., & Hassan, O. A. K. (2014). Change detection of urban heat islands and some related parameters using multi-temporal landsat images; a case study for Cairo City, Egypt. *Urban Climate*, 10, 171–188.
- Emmanuel, R., Rosenlund, H., & Johansson, E. (2007). Urban shading – A design option for the tropics? A study in Colombo, Sri Lanka. *International Journal of Climatology*, 27(14), 1995–2004.
- Erell, E., Pearlmutter, D., & Williamson, T. (2011). *Urban microclimate. Designing the spaces between buildings* (1st ed.). London: Earthscan.
- Geosampa (2016). *Mapa Digital da Cidade de São Paulo – Digital Map of São Paulo City*. Accessed 20 July, 2016 http://geosampa.prefeitura.sp.gov.br/PaginasPublicas/_SBC.aspx#.
- Google Earth, Belenzinho, Municipality of São Paulo, 23°32'21.31"S and 46°35'26.68"O, 2016. Accessed 10 July, 2016.
- Grimmond, C. S. B. (2006). Progress in measuring and observing the urban atmosphere. *Theoretical and Applied Climatology*, 84, 3–22.
- Harvey, D. (2005). *A produção capitalista do espaço* (1st ed.). São Paulo: Annablume.
- Jacobi, P. R., & Macedo, L. S. V. (2000). *Consciência cidadã e poluição atmosférica: estado de situação na cidade de São Paulo*. Santiago de Chile: CEPAL (Comisión Económica para América).
- Joshi, J. P., & Bhatt, B. (2012). Estimating temporal land surface temperature using remote sensing: A study of Vadodara urban area, Gujarat. *International Journal of Geology Earth and Environmental Sciences*, 2(1), 123–130.
- Knowles, R. L., & Berry, R. D. (1980). *Solar envelope concepts: Moderate density building applications*. Golden, Colorado: Solar Energy Research Institute SERI/SP-98155-1.
- Marx, K. (1967). *Capital*, 3 Vol. New York: International Publishers.
- Municipality of São Paulo, Law n°16.050 of 31 July 2014. Official Diary of the City of São Paulo, 1 August 2014, Accessed 14 September, 2016 <https://goo.gl/zKnVyp>.
- Newman, O. (1996). *Creating defensible space* (1st ed.). Washington: U.S. Policy Development and Research.
- Oke, T. R. (1987). *Boundary layer climate* (2nd ed.). London: Routledge.
- Oke, T. R. (2006). *Initial guidance to obtain representative meteorological observations at urban sites*. World Meteorological Organization/TD-No. 1250. Accessed 19 January, 2017 <https://pdfs.semanticscholar.org/d1d3/e2ffbed0e272073d73b0a3f6e55a3bdb372f.pdf>.
- Salingaros, N. A., & West, B. J. (1999). A universal rule for the distribution of sizes. *Environment and Planning B Planning and Design*, 26, 909–923.
- Salvati, L., Smiraglia, D., Bajocco, S., & Munafò, M. (2014). Land use changes in two Mediterranean Coastal Regions: Do urban areas matter? *International Journal of Environmental Ecological Geographical Engineering*, 8(9), 562–566.
- Soleymanpour, R., Parsaee, N., & Banaei, M. (2015). Climate comfort comparison of vernacular and contemporary houses of Iran. *Procedia Social and Behavioral Sciences*, 201, 49–61.
- Stewart, I. D., Oke, T. R., & Kravynhoff, E. S. (2014). Evaluation of the local climate zone scheme using temperature observations and model simulations. *International Journal of Climatology*, 34(4), 1062–1080.
- Suau, C., Bugarič, B., & Fikfak, A. (2015). Urban history, morphology and environmental urban design of maritime spaces in the old town of Koper. *Annals Istrian Mediterranean Studies Series History Sociology*, 25, 65–84 ISSN 1408-5348.
- Sung, H., & Oh, J.-T. (2011). Transit-oriented development in a high-density city: Identifying its association with transit ridership in Seoul, Korea. *Cities*, 28, 70–82.
- Suzuki, H., Cervero, R., & Iuchi, K. (2013). *Transforming cities with transit. Transit and land-use integration for sustainable urban development*. Washington DC: International Bank for Reconstruction and Development/The World Bank.
- Tarifa, J. R., & Armani, G. (2000). *Atlas ambiental do município de São Paulo*. Laboratório de Climatologia Departamento de Geografia/Faculdade de Filosofia, Letras e Ciências Humanas-FFCLH Universidade de São Paulo – USP. [Accessed 12 January, 2017] <http://atlasambiental.prefeitura.sp.gov.br/arquivos/As%20Unidades%20Clim%20E1ticas%20Urbanas.pdf>.
- UN-Habitat Core Team (2016). *Urbanization and development: Emerging futures*. Nairobi: United Nations Human Settlements Programme.
- Unger, J. (2004). Intra-urban relationship between surface geometry and urban heat island: Review and new approach. *Climate Research*, 27, 253–264.
- World Health Organization (WHO) (2016). *Ambient air pollution: A global assessment of exposure and burden of disease*. Geneva: WHO Press.
- Weather Station IAG-USP. (2016). <http://www.estacao.iag.usp.br/> Accessed 30 June, 2016.
- Weather Station CETESB. (2017). <http://ar.cetesb.sp.gov.br/configuracao-da-rede-automatica/> Accessed 10 January, 2017.
- Wong, N. H., Jusuf, S. K., Syafii, N. I., Chen, Y., Hajjaji, N., Sathyanarayanan, H., et al. (2011). Evaluation of the impact of the surrounding urban morphology on building energy consumption. *Solar Energy*, 85(1), 57–71.
- Xie, X., Huang, Z., Wang, J., & Xie, Z. (2005). The impact of solar radiation and street layout on pollutant dispersion in street canyon. *Building and Environment*, 40(2), 201–212.
- Yuan, C., & Ng, E. (2012). Building porosity for better urban ventilation in high-density cities—A computational parametric study. *Building and Environment*, 50, 176–189.
- Zhu, J. (2012). Development of sustainable urban forms for high-density low-income Asian countries: The case of Vietnam. *Cities*, 29, 77–87.